Antiferromagnet-induced perpendicular magnetic anisotropy in ferromagnetic/antiferromagnetic/ferromagnetic trilayers

Bo-Yao Wang,[1,*] Po-Han Lin,[1] Ming-Shian Tsai,[1] Chun-Wei Shih,[1] Meng-Ju Lee,[1] Chun-Wei Huang,[1] Nae-Yeou Jih,[2] and Der-Hsin Wei[3]

[1]*Department of Physics, National Changhua University of Education, Changhua 500 Taiwan*

[2]*The Center of Teacher Education, National Chung Hsing University, Taichung 402, Taiwan*

[3]*National Synchrotron Radiation Research Center, Hsinchu 300, Taiwan*

(Received 11 April 2016; revised manuscript received 1 June 2016; published 1 August 2016)

This study demonstrates the effect of antiferromagnet-induced perpendicular magnetic anisotropy (PMA) on ferromagnetic/antiferromagnetic/ferromagnetic (FM/AFM/FM) trilayers and reveals its interplay with a long-range interlayer coupling between separated FM layers. In epitaxially grown 12 monolayer (ML) Ni/Co/Mn/5 ML Co/Cu(001) films, magnetic hysteresis loops and element-resolved magnetic domain imaging showed that the magnetization direction of the top layers of 12 ML Ni/Co films could be changed from the in-plane direction to the perpendicular direction, when the thickness of the Mn films (t_{Mn}) was greater than a critical value close to the thickness threshold associated with the onset of AFM ordering ($t_{Mn} = 3.5$ ML). The top FM layers exhibited a significantly enhanced PMA when t_{Mn} increased further, and this enhancement can be attributed to a strengthened AFM ordering of the volume moments of the Mn films, as evidenced by the presence of induced domain frustration. By contrast, the long-range interlayer coupling presented clear effects only when t_{Mn} was at a lower coverage.

DOI: 10.1103/PhysRevB.94.064402

I. INTRODUCTION

Magnetic thin films with perpendicular magnetic anisotropy (PMA) have attracted considerable research attention because of their potential for magnetological devices achieving high density, high thermal stability, and low critical current for current-induced magnetization switching [1–4]. To generate PMA, studies have explored several approaches including fabricating noble metal Co/(Pd, Pt) or CoFeB/MgO multilayers through interfacial anisotropy [3–6] or noble-metal/transition-metal alloys through crystalline anisotropy [6,7]. However, at a reduced dimension, simultaneously satisfying both requirements of high thermal stability and low current for current-induced magnetization switching remains a challenge [3,5,8]. Using antiferromagnetic (AFM) thin films is an alternative approach for realizing PMA in ferromagnetic (FM) layers [9–14]. Recent studies on FM/Mn bilayers have demonstrated the advantages of flexibly controlling the coercivity (H_c) or thermal stability of PMA by varying the thickness of AFM films [10] or inserting an ultrathin FM layer through the magnetic proximity effect [12]. Although a clear effect has been shown in FM/AFM bilayers [9–14], the effects on magnetic thin films with trilayer or multilayer structures, which are closer to the application of state-of-the-art perpendicular-based magnetoresistance or spin-transfer torque devices, are still unclear.

In an FM/AFM/FM trilayer, the long-range type Ruderman-Kittel-Kasuya-Yosida (RKKY) coupling as well as the magnetostatic coupling can occur and affect the relative magnetic orientation between separated FM layers [15–20]. For example, if the intrinsic magnetic anisotropy levels of two separated FM layers are different, the long-range interlayer coupling can line the magnetic easy axis of the FM layer with weak magnetic anisotropy in the direction of the FM layer exhibiting strong magnetic anisotropy [17,18]. Once the space layer is replaced by the AFM layer, long-range interlayer coupling as well as short-range FM-AFM exchange coupling can occur and affect the magnetic anisotropy of the FM layers [19–22]. Therefore, when the effect of antiferromagnet-induced PMA on FM/AFM/FM trilayers or multilayers is to be determined, the interplay of the short-range FM-AFM exchange coupling with the long-range interlayer coupling, in terms of the influence on the magnetic anisotropy of FM layers, must be investigated.

Among various antiferromagnets, face-centered-cubic-like Mn thin films are considered attractive systems because these films can be fabricated using current epitaxial growth techniques [23–33]. Notably, a recent study demonstrated that expanded face-centered-tetragonal (e-fct) Mn films can engender an antiferromagnet-induced PMA phenomenon in adjacent FM layers at room temperature [14]. In the present work, 12 monolayer (ML) Ni/Co/e-fct Mn/5 ML Co films were prepared as a model system for realizing and investigating antiferromagnet-induced PMA in FM/AFM/FM trilayers. The system exhibits stable in-plane magnetic anisotropy (IMA) for one FM layer (5 ML Co film) but tunable magnetic anisotropy for another FM layer (12 ML Ni/Co film) [14,25], rendering it suitable for probing Mn-film-induced magnetic anisotropy and its interplays with long-range interlayer coupling in the present FM/AFM/FM trilayers.

In this study, we observed that antiferromagnet-induced perpendicular magnetization could be realized in 12 ML Ni/Co/Mn/5 ML Co/Cu(001) FM/AFM/FM trilayered films. We determined that perpendicular magnetization could be established in the top 12 ML Ni/Co films when the thickness of the Mn films (t_{Mn}) was greater than a value close to the critical thickness associated with the onset of AFM ordering

*bywang1735@cc.ncue.edu.tw

($t_{Mn} = 3.5$ ML). We also observed a significantly enhanced PMA of the top FM layers when t_{Mn} was increased further, and this enhancement can be attributed to a strengthened AFM ordering of the volume moments of the Mn films, as evidenced by the presence of induced domain frustration. By contrast, the long-range interlayer coupling presented clear effects only when t_{Mn} was at a lower coverage.

II. EXPERIMENT

In this study, 12 ML Ni/0-3 ML Co/Mn/5 ML Co films were prepared and investigated *in situ* in an ultrahigh-vacuum preparation chamber with a base pressure of 2×10^{-10} Torr. Cu(001) single-crystal substrates with a 0.1° miscut were cleaned through cycles of 2-keV Ar^+ ion sputtering and annealed at 800 K for 5 min to obtain a smooth morphology and a well-ordered crystalline structure [34,35]. The growth rates were monitored through medium energy electron diffraction (MEED). As shown in Fig. 1, a layer-by-layer growth mode was observed for Co films grown on Cu(001), Mn films grown on 5 ML Co layers, and Ni films grown on Co/2, 8 ML Mn/5 ML Co/Cu(001). Uniform films or films with wedge-shaped Mn layers were deposited on the substrates for analyzing the crystalline structure and magnetic hysteresis loops or magnetic domain images of the samples.

The average in-plane ($d_{\parallel}$) and interlayer distances ($d_{\perp}$) of the films were determined through low energy electron diffraction (LEED) with kinematic approximation (LEED I/V) [35]. As presented in the Supplemental Material [36], the average $d_{\parallel}$ and $d_{\perp}$ of the 12 ML Ni films grown on 1–3 ML Co/1–8 ML Mn/5 ML Co films were similar to the values of Ni films grown on Cu(001) [37,38]. On the other hand, the c/a ratio of the Mn films stabilized at approximately 1.05 ($t_{Mn} > 4$ ML). This indicates the presence of the e-fct structure in the Mn films, which is consistent with the findings of experimental studies [27,29] and a theoretical calculation [39].

The magnetic hysteresis loops of the thin films were measured on the basis of the magneto-optical Kerr effect (MOKE) in both longitudinal and polar geometries. The magnetic domain images of the films were obtained *in situ* through photoemission electron microscopy (PEEM) [40–42] by observing the x-ray magnetic circular dichroism (XMCD) effects at beamline BL05B2 of the National Synchrotron Radiation Research Center, Hsinchu, Taiwan. The angles of the incident right circularly polarized (RCP) x rays were 0° relative to the in-plane [0$\bar{1}$0] crystallographic direction of Cu(001) and 25° relative to the surface plane. The magnetic information of individual elements can be obtained from the asymmetry of the XMCD curve at the $L_{3,2}$ absorption edges [43]. The full-field view of a magnetic domain image was resolved by recording the secondary electrons emitted from the magnetic sample through PEEM. Contrast normalization was achieved by performing imaging calculations for the two full-field images captured at the Ni or Co L_3 and L_2 edges by applying the formula $(I_{L3} - I_{L2})/(I_{L3} + I_{L2})$ [43,44], where I_{L3} and I_{L2} are the x-ray absorption intensities of the sample at the L_3 and L_2 edges, respectively. In this study, magnetic imaging was performed under the as-grown condition at 300 K.

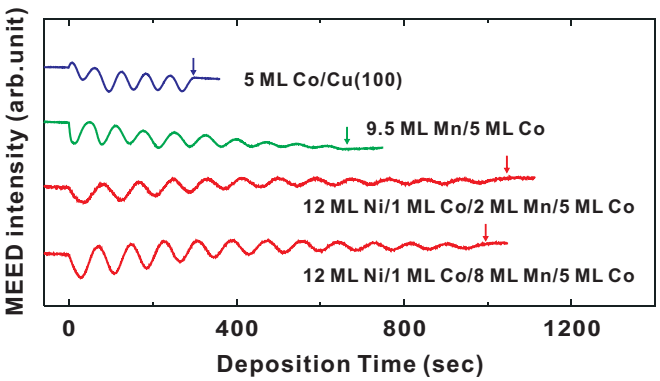

FIG. 1. Selected medium energy electron diffraction (MEED) (0,0) beam intensity curves as functions of deposition time for the Co films grown on Cu(001), Mn films grown on 5 ML Co/Cu(001), and Ni films grown on 1 ML Co/2, 8 ML Mn/5 ML Co/Cu(001) at 300 K. The thickness of the films was calibrated through the oscillation in MEED curves. The arrows indicate the time for closing the shutter.

III. RESULTS

A. Magnetic properties of the 12 ML Ni/Co and Mn/5 ML Co/Cu(001) films

The magnetic properties of the 12 ML Ni/Co and Mn/5 ML Co/Cu(001) films, constituting the top and bottom components, respectively, of the FM/AFM/FM trilayers in this study, were first characterized through the MOKE. Figure 2(a) shows the magnetic hysteresis loops of the 12 ML Ni/0–3 ML Co films measured along the in-plane [100] and out-of-plane [001] directions at 300 K. The 12 ML Ni films demonstrated a characteristic PMA, which was contributed by the perpendicular magnetocrystalline anisotropy of the films [45–47]. When the Co films were included as an underlayer of the Ni films, the magnetic anisotropy of the composite FM layers was changed from the perpendicular direction to the in-plane direction. This spin-reorientation transition (SRT) was induced by the in-plane-oriented shape anisotropy as well as magnetocrystalline anisotropy of the Co films [47]. Therefore, the 12 ML Ni/1–3 ML Co films exhibiting tunable IMA are proven to be flexible probing layers for investigating the antiferromagnet-induced PMA in the present FM/AFM/FM trilayers. Figure 2(b) shows the magnetic hysteresis loops of the Mn/5 ML Co/Cu(001) films, which are the bottom components of the present FM/AFM/FM trilayers. Because the 5 ML Co/Cu(001) films revealed strong IMA [34,35], their magnetic anisotropy remained in the in-plane direction when the Mn films were deposited. Notably, the in-plane H_c was significantly enhanced when $t_{Mn} > 4.0$ ML. According to previous studies [43,48–53], the enhanced H_c in the AFM/FM bilayers could be attributed to an establishment of AFM ordering as well as AFM-FM exchange coupling. Therefore, the threshold for the onset of AFM ordering of the Mn films in Mn/5 ML Co/Cu(001) was estimated to be 4.0–4.5 ML. This value is consistent with that of a previous study [26]. The hysteresis feature of Mn/5 ML Co/Cu(001) completely disappeared when $t_{Mn} > 6.5$ ML (not shown in the figure). This behavior can be attributed to a high H_c value, where the magnetic field cannot saturate the magnetization of films.

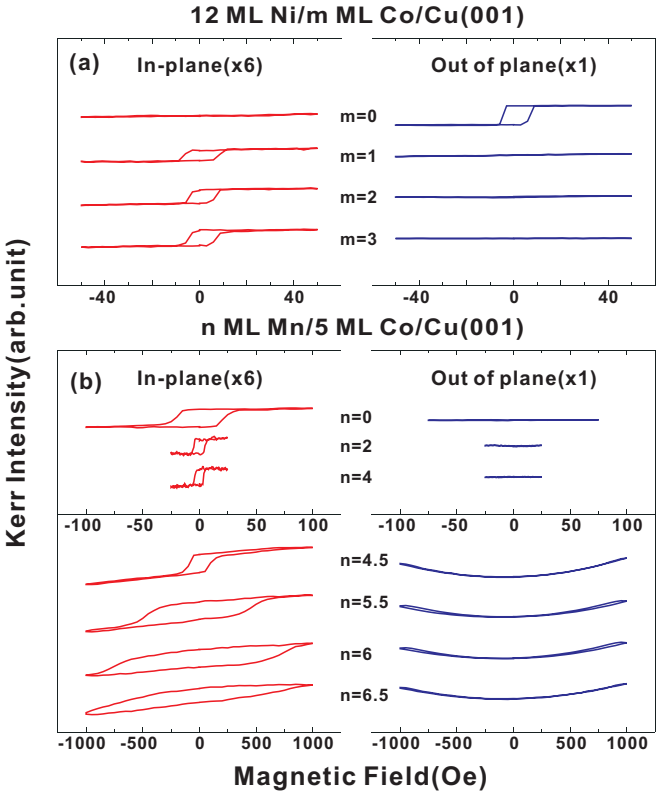

FIG. 2. In-plane and out-of-plane magnetic hysteresis loops of (a) 12 ML Ni/0-3 ML Co/Cu(001) and (b) 0–6.5 ML Mn/5 ML Co/Cu(001). In (a), the magnetic easy axis of the FM films is changed from the perpendicular to the in-plane direction when the 1–3 ML Co film is included. In (b), the magnetic easy axis of 0–6.5 ML Mn/5 ML Co bilayers remains in the in-plane direction when a significant coercivity (H_c) enhancement is observed for $t_{Mn} > 4$ ML. The hysteresis feature disappears when $t_{Mn} > 6.5$ ML (not shown in figure), and this is probably induced by a strongly enhanced H_c of the films.

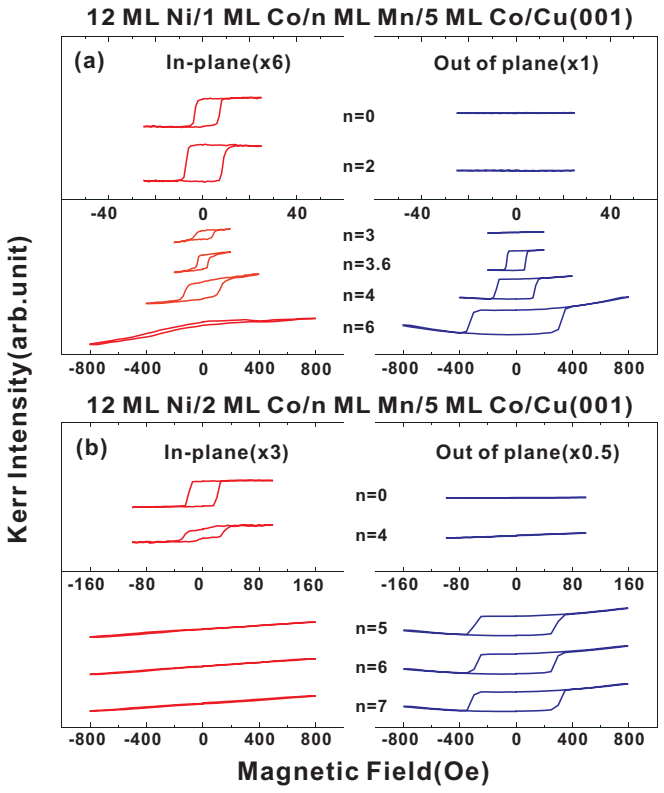

FIG. 3. In-plane and out-of-plane magnetic hysteresis loops of (a) 12 ML Ni/1 ML Co/Mn/5 ML Co/Cu(001) and (b) 12 ML Ni/2 ML Co/Mn/5 ML Co/Cu(001) films as functions of t_{Mn} measured at room temperature. Perpendicular magnetization is observed when t_{Mn} is greater than a critical thickness that depends on the thickness of the Co films at the top.

B. Induced SRT in the 12 ML Ni/Co/Mn/5 ML Co/Cu(001) films

When the 12 ML Ni/Co and Mn/5 ML Co films were combined into FM/AFM/FM trilayers, the magnetic anisotropy of the films changed significantly. Figure 3(a) illustrates the magnetic hysteresis loops of 12 ML Ni/1 ML Co/Mn/5 ML Co/Cu(001) films. The films exhibited stable IMA when t_{Mn} was at a low coverage and then revealed coexisting in-plane and perpendicular magnetization when t_{Mn} reached 3.6 ML. When $t_{Mn} > 4$ ML, only perpendicular magnetization was measured. A similar behavior was also observed in 12 ML Ni/2 ML Co/Mn/5 ML Co/Cu(001) [Fig. 3(b)], in which the critical thickness associated with the onset of PMA was measured to be approximately 5 ML.

To characterize the presence of perpendicular magnetization when SRT occurs, the magnetic hysteresis loops of the present FM/AFM/FM films were compared with those of the top or bottom components of the films. Directly comparing the perpendicular magnetization between the 12 ML Ni/Co/Mn/5 ML Co/Cu(001) and 12 ML Ni/Co/Cu(001) films was unlikely because the 12 ML Ni/Co/Cu(001) films exhibited only IMA [Fig. 2(a)]. Instead, we compared the perpendicular magnetic hysteresis loops of 14 ML Ni/1 ML Co/6 ML Mn/5 ML Co/Cu(001) and 14 ML Ni/1 ML Co/Cu(001), where providing an additional 2 ML Ni film to both systems enhanced the PMA through an increased perpendicular crystalline anisotropy. Figure 4(a) indicates that the perpendicular magnetization magnitudes of both films are similar. This suggests that the perpendicular magnetization of 14 ML Ni/1 ML Co/6 ML Mn/5 ML Co/Cu(001) could be contributed by the top FM layer (14 ML Ni/1 ML Co). Therefore, the perpendicular magnetization measured in the 12 ML Ni/Co/Mn/5 ML Co/Cu(001) films [Figs. 3(a) and 3(b)] could also be contributed by the top 12 ML Ni/Co films.

As shown in the magnetic hysteresis loops in Fig. 2(a), 12 ML Ni/1 ML Co/3.6–4.0 ML Mn/5 ML Co/Cu(001) films presented coexisting perpendicular and in-plane magnetization. Nevertheless, the in-plane magnetization disappeared when t_{Mn} was increased further. To characterize the presence of in-plane magnetization and trace its evolution when t_{Mn} was increased, the in-plane magnetic hysteresis loops of 12 ML Ni/1 ML Co/4 ML Mn/5 ML Co/Cu(001) and 4 ML Mn/5 ML Co/Cu(001) films were compared. Figure 4(b) indicates that the in-plane magnetization magnitudes of both films are at the same level. This suggests that the in-plane magnetization observed in the 12 ML Ni/1 ML Co/4 ML Mn/5

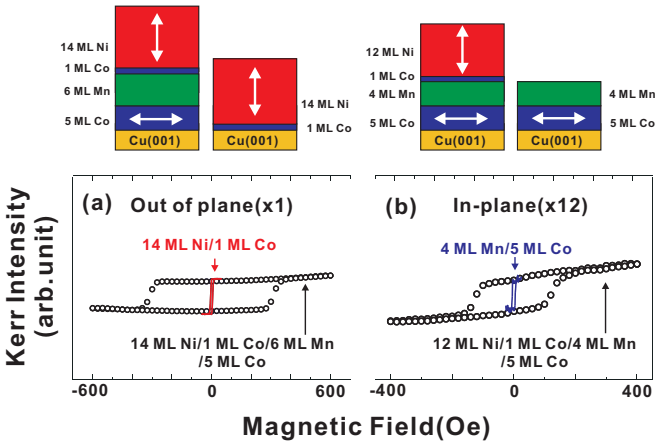

FIG. 4. (a) Out-of-plane magnetic hysteresis loops of 14 ML Ni/1 ML Co/6 ML Mn/5 ML Co/Cu(001) and 14 ML Ni/1 ML Co/Cu(001). (b) In-plane magnetic hysteresis loops of 12 ML Ni/1 ML Co/4 ML Mn/5 ML Co/Cu(001) and 4 ML Mn/5 ML Co/Cu(001). A comparison of magnetization in magnetic hysteresis loops of (a) and (b) suggests that the perpendicular and in-plane magnetization of the 12 ML Ni/Co/Mn/5 ML Co/Cu(001) films when the SRT occurs could be contributed by the top (12 ML Ni/Co) and bottom (5 ML Co) layers, respectively.

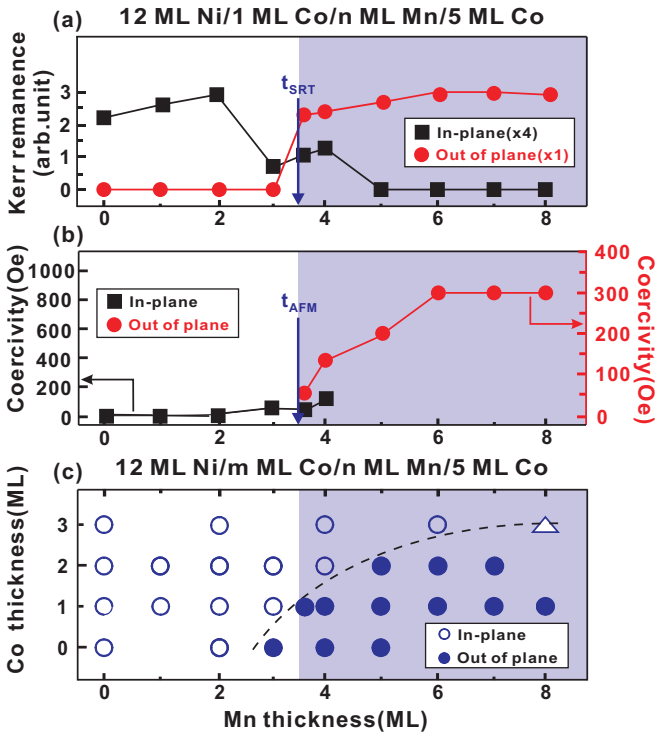

FIG. 5. (a) In-plane and perpendicular remanent magnetization of 12 ML Ni/1 ML Co/Mn/5 ML Co/Cu(001) as a function of t_{Mn} measured at 300 K. (b) H_c of in-plane and out-of-plane hysteresis loops of 12 ML Ni/1 ML Co/Mn/5 ML Co/Cu(001) as a function of t_{Mn}. In (a) and (b), the thicknesses associated with the onset of SRT and AFM ordering of Mn films in 12 ML Ni/1 ML Co/Mn/5 ML Co/Cu(001) are indicated by t_{SRT} and t_{AFM}, respectively. (c) Magnetic easy axis phase diagram of the top FM layers in 12 ML Ni/0-3 ML Co/0-8 ML Mn/5 ML Co/Cu(001) measured according to the longitudinal and polar magneto-optical Kerr effect (MOKE) at 300 K. The dashed line represents the boundary between in-plane and perpendicular magnetization.

ML Co/Cu(001) films could be contributed by the bottom 5 ML Co films. According to this knowledge, a disappearance of in-plane magnetization when t_{Mn} was further increased [Figs. 3(a) and 3(b)] could also be associated with a strongly enhanced H_c, similar to the behavior of the Mn/5 ML Co/Cu(001) films [Fig. 2(b)] and correlated with an establishment of AFM ordering of the Mn films. According to the aforementioned comparisons of magnetic hysteresis loops, we can conclude that an establishment of perpendicular magnetization in 12 ML Ni/1–2 ML Co/Mn/5 ML Co/Cu(001) films is contributed by the top FM layers (12 ML Ni/Co films). Moreover, the magnetization of the bottom Co films remains in the in-plane direction when t_{Mn} is increased, although the hysteresis feature could disappear because of the strongly enhanced H_c value.

C. Origin of induced PMA in the 12 ML Ni/Co/Mn/5 ML Co/Cu(001) films

The aforementioned results revealed that perpendicular magnetization of the top 12 ML Ni/Co films could be induced in the 12 ML Ni/Co/Mn/5 ML Co/Cu(001) films. To further elucidate the correlation between the establishment of the PMA of the FM films and the antiferromagnetism of the Mn films, the behavior of SRT was compared with the variation in the H_c value of the magnetic films as a function of t_{Mn}. We used H_c for this comparison for two reasons. First, an enhanced H_c is typically accepted as a standard indicator of the establishment of an AFM-FM exchange coupling as well as AFM ordering in AFM/FM bilayers [43,48–53]. Second, according to previously reported systems showing an antiferromagnet-induced PMA, [11,14] the presence of PMA is associated with the establishment of a perpendicular crystalline anisotropy of the unpinned moments of the AFM films at the interface. These moments trigger strong H_c enhancement in perpendicular magnetic hysteresis loops [11]. Therefore, we expected to observe a similar behavior in the present FM/AFM/FM trilayers, if the mechanism triggering PMA is the same as that determined for the previously reported AFM/FM bilayers. [11,14] In the present study, the system comprising the 12 ML Ni/1 ML Co/Mn/5 ML Co/Cu(001) films was selected for the comparison, because the top FM layers of the 12 ML Ni/1 ML Co films revealed weak IMA, which could be extremely sensitive to the probing of the effects induced by the adjacent Mn films.

Figure 5(a) illustrates the remanent magnetization of the hysteresis loops of the 12 ML Ni/1 ML Co/0-8 ML Mn/5 ML Co/Cu(001) films. According to the evolution of in-plane and out-of-plane remanent magnetization displayed in this figure, the critical thickness associated with the onset of SRT (t_{SRT}) was estimated to be 3.5 ML. In particular, as shown in Fig. 5(b), the H_c value was significantly enhanced when t_{Mn} approached the same value of 3.5 ML ($t_{AFM} = 3.5$ ML). Therefore, the presence of PMA in the top FM layers and the establishment of an AFM ordering of the Mn films were associated with the same critical thickness, thus proving the mechanism of antiferromagnet for triggering the PMA in the

present FM/AFM/FM systems. Moreover, the estimated t_{AFM} value (3.5 ML) in 12 ML Ni/1 ML Co/Mn/5 ML Co/Cu(001) was slightly lower than that (4.0–4.5 ML) in Mn/5 ML Co/Cu(001) [Fig. 2(b)]. The smaller value of t_{AFM} in 12 ML Ni/1 ML Co/Mn/5 ML Co/Cu(001) could be attributed to the establishment of a stronger AFM ordering of the Mn films in the FM/AFM/AM trilayers, and this is because of the contribution of magnetic proximity effects from the top FM layers [19,54–56].

The preceding results were further compared with a magnetic easy axis phase diagram, which summarizes a general feature of the magnetic anisotropy of the top FM layers in 12 ML Ni/0–3 ML/0–8 ML Mn/5 ML Co/Cu(001). As shown in Fig. 5(c), the threshold t_{Mn} for achieving PMA shifted from 3.5 to 8 ML when the thickness of a Co film in the top FM layers increased from 1 to 3 ML. Such a behavior is attributed to an enhancement of the IMA of the 12 ML/Ni/Co films when the thickness of the Co film increased [Fig. 2(a)], where PMA must be triggered by a thicker Mn film with stronger AFM ordering. Moreover, this tendency revealed a competition mechanism between the IMA of the top FM layers and the PMA induced by the AFM Mn layer. Apart from the aforementioned cases, in the 12 ML Ni/Mn/5 ML Co/Cu(001) films, the top Ni layers exhibited PMA intrinsically. The presence of IMA in Ni films when t_{Mn} was at a low coverage is attributed to direct exchange coupling or indirect interlayer coupling between the top and bottom FM layers, similar to the case of previously reported Ni/Cu/Co trialyers [17,18]. The presence of PMA when $t_{Mn} > 2$ ML is attributed to a decoupling between the top Ni and bottom Co layers, and this is because the strength of the long-range interlayer coupling could usually be reduced when the spacer thickness was increased [18].

D. Observation of long-range interlayer coupling and antiferromagnet-induced magnetic frustration through magnetic domain imaging

To further examine the possible effects of long-range interlayer coupling and antiferromagnet-induced phenomena on the FM/AFM/FM trilayers, element-resolved XMCDPEEM measurements were performed. Magnetic domain imaging was applied to 12 ML Ni/1 ML Co/Mn/5 ML Co/Cu(001) with wedge-shaped Mn layers (Fig. 6, top left panel), and this is because the magnetic anisotropy and interlayer coupling of films could be sensitive to a variation in the Mn layer thickness. Figures 6(a) and 6(c) depict the Ni and Co domain images of the 12 ML Ni/1 ML Co/wedge-shaped 2.5–3.5 ML Mn/5 ML Co/Cu(001) films, respectively. The Ni and Co domains demonstrated similar features when $t_{Mn} < 3.0$ ML, indicating the existence of a parallel alignment of magnetization between the top Ni/Co and bottom Co layers. An inverse contrast in the Ni and Co domains was observed when $t_{Mn} > 3.0$ ML, indicating that the magnetization between the top and bottom magnetic layers exhibited an antiparallel alignment. Notably, the measurements of the magnetic hysteresis loops also revealed features of antiparallel alignment. For instance, we observed a significantly reduced magnitude of the Kerr signal of 12 ML Ni/1 ML Co/3 ML Mn/5 ML Co/Cu(001) [Fig. 3(a)], compared with that of the films when $t_{Mn} = 0$, 2, 3.6, 4 ML, suggesting an antiparallel alignment of magnetization between

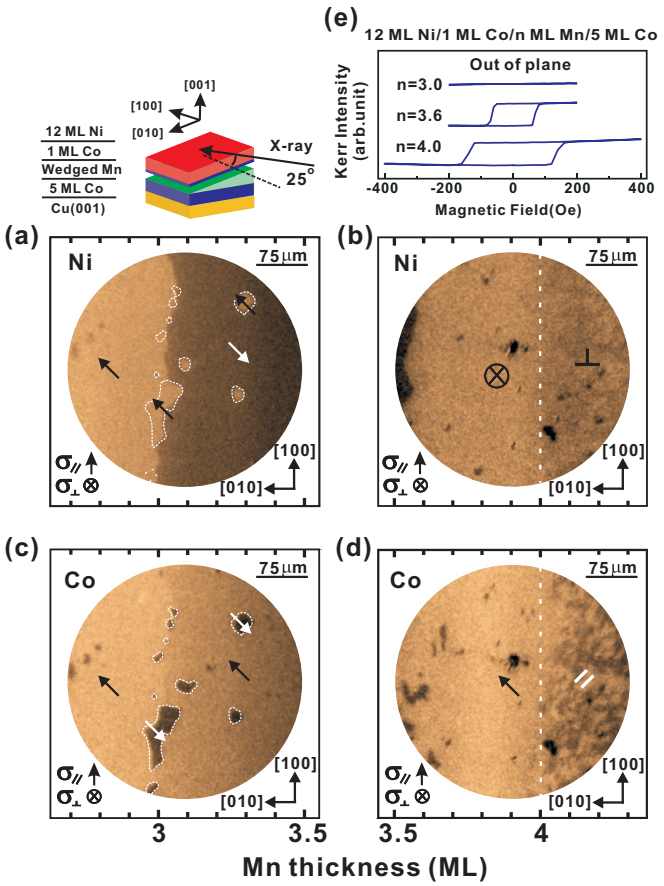

FIG. 6. (a) and (b): Ni domain images of the 12 ML Ni/1 ML Co/wedge-shaped Mn/5 ML Co/Cu(001) films; (c) and (d): Co domain images of the 12 ML Ni/1 ML Co/wedge-shaped Mn/5 ML Co/Cu(001) films obtained with right circularly polarized x-rays at 300 K; (e) out-of-plane magnetic hysteresis loops of 12 ML Ni/1 ML Co/3-4 Mn/5 ML Co/Cu(001). In (a)–(d), $\sigma_{\parallel}$ and $\sigma_{\perp}$ at the bottom left denote the horizontal and vertical components of the photohelicity of the incident x-ray with respect to the sample, as illustrated in the top left-most region. The magnetization directions of the magnetic domains are indicated by the black/white or up/down arrows. In (b) and (d), the dashed lines represent the boundaries for the onset of frustration of the Ni or Co domain. In areas presenting domain frustration, the magnetization directions are indicated by $\perp$ or $\parallel$. In (c) and (d), the bottom 5 ML Co film contributes approximately 75–70% of the total Co signal when $t_{Mn} = 3-4$ ML, according to an analysis of the electron yield sampling depth [43]. The feature of the Co domain image is therefore mainly contributed by the bottom Co film.

the top and bottom FM layers if the interlayer coupling is strong and the H_c values for the top and bottom FM layers are similar [57]. Moreover, 12 ML Ni/2 ML Co/4 ML Mn/5 ML Co/Cu(001) [Fig. 3(b)] showed a two-step hysteresis loop feature, where a reduced magnitude of the Kerr signal in the remanent state is attributed to an antiparallel coupling between the top and bottom FM layers. As shown in Figs. 6(b) and 6(d), the collinear type coupling (i.e., parallel or antiparallel) between the top and bottom FM layers disappeared when $t_{Mn} > 3.5$ ML. However, the magnetization direction of the top layers of the 12 ML Ni/Co films changed to the

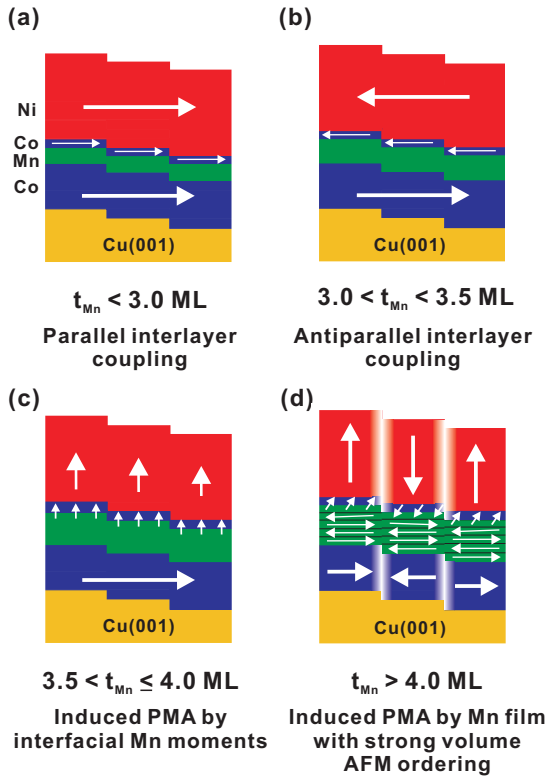

FIG. 7. Schematic magnetic orientations of 12 ML Ni/1 ML Co/Mn/5 ML Co/Cu(001) as a function of t_{Mn}, according to the results of MOKE and PEEM. A single atomic step is used in the model of thin films for simulating the presence of interface roughness inherent in the grain boundary or terrace of substrates. The interfacial magnetic moments and volume AFM spin ordering of Mn films in models have been presented by previous studies [14,32].

perpendicular direction according to the results of the MOKE [Fig. 6(e)].

Notably, the size of both the Ni and Co domains was significantly reduced when t_{Mn} reached 4.0 ML. According to previous studies [26,58], the presence of domain frustration in FM films could be induced by an exchange coupling with an AFM layer presenting frustrated spin alignment at the AFM-FM interface. Such a behavior could also be present in the case of the FM/e-fct Mn films with an appropriately-defined layered spin structure [32,33] and strong lateral exchange coupling [26] of AFM films, when the presence of a step or terrace inherent in the substrate is considered. As illustrated in Fig. 7(d), the robust lateral long-range spin ordering of the volume of the e-fct Mn films could engender the formation of a twin-phase spin arrangement of the Mn films at the AFM-FM interface, which could substantially reduce the domain size of the adjacent FM layers because of the established collinear and biquadratic coupling at this interface. The phenomenon of induced domain frustration is expected to be exhibited when the AFM ordering of the volume moments of AFM films is well established; therefore, in this study, the feature of the induced domain frustration clearly demonstrated a well-established AFM ordering of the volume moments of the e-fct Mn films when t_{Mn} reached 4 ML.

IV. DISCUSSION

A. Contribution of the volume moments of Mn films on the antiferromagnet-induced PMA

According to the results of this study, the e-fct Mn films result in domain frustration in both the top and bottom FM layers [Figs. 6(b) and 6(d)]. In particular, the critical thickness for triggering the domain frustration (approximately 4.0 ML) is slightly higher than the threshold thickness associated with the presence of PMA in the top FM layers (>3.5 ML) [Fig. 6(e)]. This difference can be associated with the different origins of the magnetic moments of the AFM films. According to previous studies, the established PMA of FM films is generated by the unpinned moments of an AFM layer at the interface, and the strength can be enhanced or reduced through an exchange interaction with the volume moments of the AFM film [11,14]. By contrast, the behavior of antiferromagnet-induced domain frustration is expected to be triggered when the long-range AFM ordering of the volume of Mn films is well established [26]. Therefore, the t_{Mn} threshold for the formation of domain frustration in FM films is likely to occur at a higher value than that associated with the presence of PMA because of the influence of finite-size effects [59]. In the present study, the behavior of antiferromagnet-induced domain frustration occurred concurrently with the presence of a strongly enhanced PMA in the top FM layers. These volume moments of the Mn films with an established AFM ordering possibly enhance the strength of the PMA of the interfacial AFM moments as well as the top FM layers through noncollinear exchange coupling [11,14]. Therefore, the results of this study confirm the interface exchange coupling behavior of the antiferromagnet-induced PMA; moreover, we demonstrate the effect of the volume moments of the AFM films on the FM/AFM/FM trilayers. This information provides a deeper insight into the behavior of antiferromagnet-induced PMA.

B. Competition of long-range interlayer coupling and antiferromagnet-induced PMA

Figure 7 presents a summary of the effects of the long-range interlayer coupling and antiferromagnet-induced PMA in 12 ML Ni/1 ML Co/Mn/5 ML Co/Cu(001) as a function of t_{Mn}. The long-range interlayer coupling, which could be attributed to RKKY or magnetostatic coupling, occurred when t_{Mn} < 3.5 ML [Figs. 7(a) and 7(b)]. Perpendicular magnetization was observed in the top FM layers when t_{Mn} > 3.5 ML [Fig. 7(c)], where the establishment of the AFM ordering of the Mn films started. Notably, as shown in the magnetic hysteresis loops [Fig. 3] and magnetic domain images [Fig. 6], the long-range interlayer coupling showed clear effects only when t_{Mn} was at a low coverage, before the presence of PMA in the top FM layers and the establishment of an AFM ordering of the Mn films. Such a phenomenon could be attributed to two possible reasons. First, the energy of long-range interlayer coupling reported in conventional FM/non-FM/FM trilayer systems is in the order of magnitude of approximately 0.01–0.1 meV/atom (spacer thickness of approximately 3–4 ML) [18]. Such a value is considerably lower than the exchange energy responsible for the AFM-induced PMA (3–4 meV/atom) [9,11,14]. Moreover,

for the RKKY-type interlayer coupling, the energy could be significantly reduced when the thickness of the spacer layer increased [18]. By contrast, the AFM ordering as well as AFM-FM exchange coupling were enhanced when t_{Mn} increased, and this is due to the finite-size effects of magnetic materials [59]. Therefore, once the AFM ordering of Mn films as well as the PMA are established, the long-range interlayer coupling is unlikely to overcome the AFM-FM exchange coupling and line the magnetization of the top layers of 12 ML Ni/Co films back to the in-plane direction. Second, according to previous studies, the spin configuration of e-fct Mn films is proven to be an in-plane layered structure [32,33]. In 12 ML Ni/1 ML Co/Mn/5 ML Co/Cu(001), Mn films with highly localized in-plane-oriented AFM moments may not be a favorable medium for transmitting an RKKY coupling between in-plane magnetic Co films at the bottom and perpendicular magnetic Ni/Co films at the top. Therefore, once the AFM ordering of the Mn films as well as the PMA are established, the direct exchange-coupling-assisted antiferromagnet-induced PMA can become a dominant phenomenon in FM/AFM/FM trilayers. Such knowledge is crucial for further generalizing the effects of AFM-induced PMA on FM/AFM/FM trilayers or multilayers for application in future perpendicular-based magnetic devices.

V. CONCLUSION

We successfully realized antiferromagnet-induced PMA in a series of 12 ML Ni/Co/Mn/5 ML Co/Cu(001) films and demonstrated its interplay with the long-range exchange coupling between separated FM layers. The results clearly indicate that the direct exchange-coupling-assisted antiferromagnet-induced PMA could overcome the long-range interlayer coupling to be a dominant phenomenon in the FM/AFM/FM exchange-coupled systems. Moreover, comparing magnetic domain images and magnetic hysteresis loops reveals the influence of the volume moments of AFM films on the effects of antiferromagnet-induced PMA. The investigation results improve the understanding of AFM-induced PMA in FM/AFM/FM layers and can facilitate the development of next-generation perpendicular-based spintronic devices.

ACKNOWLEDGMENT

This work was partly supported by the Ministry of Science and Technology, Taiwan (Grant No. MOST 102-2112-M-018-006-MY3).

[1] S. Mangin, D. Ravelosona, J. A. Katine, M. J. Carey, B. D. Terris, and E. E. Fullerton, Nat. Mater. **5**, 210 (2006).
[2] Y. Shiroishi, K. Fukuda, I. Tagawa, H. Iwasaki, S. Takenoiri, H. Tanaka, H. Mutoh, and N. Yoshikawa, IEEE Trans. Magn. **45**, 3816 (2009).
[3] S. Ikeda, K. Miura, H. Yamamoto, K. Mizunuma, H. D. Gan, M. Endo, S. Kanai, J. Hayakawa, F. Matsukura, and H. Ohno, Nat. Mater. **9**, 721 (2010).
[4] D. C. Worledge, G. Hu, D. W. Abraham, J. Z. Sun, P. L. Trouilloud, J. Nowak, S. Brown, M. C. Gaidis, E. J. Ó Sullivan, and R. P. Robertazzi, Appl. Phys. Lett. **98**, 022501 (2011).
[5] K. Yakushiji, T. Saruya, H. Kubota, A. Fukushima, T. Nagahama, S. Yuasa, and K. Ando, Appl. Phys. Lett. **97**, 232508 (2010).
[6] M. T. Johnsony, P. J. H. Bloemenzx, F. J. A. den Broedery and J. J. de Vries, Rep. Prog. Phys. **59**, 1409 (1996).
[7] G. Kim, Y. Sakuraba, M. Oogane, Y. Ando, and T. Miyazaki, Appl. Phys. Lett. **92**, 172502 (2008).
[8] J. C. Slonczewski, J. Magn. Magn. Mater. **159**, L1 (1996).
[9] B. Y. Wang, N. Y. Jih, W. C. Lin, C. H. Chuang, P. J. Hsu, C. W. Peng, Y. C. Yeh, Y. L. Chan, D. H. Wei, W. C. Chiang, and M. T. Lin, Phys. Rev. B **83**, 104417 (2011).
[10] N. Y. Jih, B. Y. Wang, Y. L. Chan, D. H. Wei, and M. T. Lin, Appl. Phys. Express **5**, 063008 (2012).
[11] B. Y. Wang, J. Y. Hong, K. H. Ou Yang, Y. L. Chan, D. H. Wei, H. J. Lin, and M. T. Lin, Phys. Rev. Lett. **110**, 117203 (2013).
[12] B. Y. Wang, C. C. Chiu, W. C. Lin, and M. T. Lin, Appl. Phys. Lett. **103**, 042407 (2013).
[13] P. Kuświk, P. L. Gastelois, M. M. Soares, H. C. N. Tolentino, M. De Santis, A. Y. Ramos, A. D. Lamirand, M. Przybylski, and J. Kirschner, Phys. Rev. B **91**, 134413 (2015).
[14] B.-Y. Wang, P.-H. Lin, M.-S. Tsai, C.-W. Shih, M.-J. Lee, C.-W. Huang, N.-Y. Jih, P.-Y. Cheng, and D.-H. Wei, Phys. Rev. B **92**, 214435 (2015).
[15] K. Binder and A. P. Young, Rev. Mod. Phys. **58**, 801 (1986).
[16] Z. Q. Qiu and N. V. Smith, J. Phys.: Condens. Matter **14**, R169 (2002).
[17] D. H. Wei, X. Y. Xu, L. F. Yin, G. S. Dong, and X. F. Jin, Phys. Rev. B **80**, 092403 (2009).
[18] W. Kuch, X. Gao, and J. Kirschner, Phys. Rev. B **65**, 064406 (2002).
[19] B. Zhang, C. B. Wu, and W. Kuch, J. Appl. Phys. **115**, 233915 (2014).
[20] C. H. Wang, Y. Y. Huang, and W. C. Lin, J. Appl. Phys. **109**, 103908 (2011).
[21] A. Tan, J. Li, C. A. Jenkins, E. Arenholz, A. Scholl, C. Hwang, and Z. Q. Qiu, Phys. Rev. B **88**, 104404 (2013).
[22] B. Sanyal, C. Antoniak, T. Burkert, B. Krumme, A. Warland, F. Stromberg, C. Praetorius, K. Fauth, H. Wende, and O. Eriksson, Phys. Rev. Lett. **104**, 156402 (2010).
[23] J. T. Kohlhepp and W. J. M. de Jonge, Phys. Rev. Lett. **96**, 237201 (2006).
[24] J. T. Kohlhepp, H. Wieldraaijer, and W. J. M. de Jonge, Appl. Phys. Lett. **89**, 032507 (2006).
[25] J. T. Kohlhepp, J. Phys. D: Appl. Phys. **40**, 1300 (2007).
[26] B.-Y. Wang, J.-Y. Hong, N.-Y. Jih, K.-H. Ou Yang, L.-R. Chen, H.-J. Lin, Y.-L. Chan, D.-H. Wei, and M.-T. Lin, Phys. Rev. B **90**, 224424 (2014).
[27] W. C. Lin, T. Y. Chen, L. C. Lin, B. Y. Wang, Y. W. Liao, K. J. Song, and M. T. Lin, Phys. Rev. B **75**, 054419 (2007).
[28] C. S. Tian, Z. Tian, J. Wu, G. S. Dong, X. F. Jin, Y. Z. Wu, and Z. Q. Qiu, J. Magn. Magn. Mater. **286**, 497 (2005).

[29] B. Schirmer, B. Feldmann, A. Sokoll, Y. Gauthier, and M. Wuttig, Phys. Rev. B **60**, 5895 (1999).
[30] T. K. Yamada, M. M. J. Bischoff, G. M. M. Heijnen, T. Mizoguchi, and H. van Kempen, Phys. Rev. Lett. **90**, 056803 (2003).
[31] U. Schlickum, N. Janke-Gilman, W. Wulfhekel, and J. Kirschner, Phys. Rev. Lett. **92**, 107203 (2004).
[32] P. J. Hsu, C. I. Lu, Y. H. Chu, B. Y. Wang, C. B. Wu, L. J. Chen, S. S. Wong, and M. T. Lin, Phys. Rev. B **85**, 174434 (2012).
[33] C. B. Wu, J. Song, and W. Kuch, Appl. Phys. Lett. **101**, 012404 (2012).
[34] M. T. Lin, W. C. Lin, C. C. Kuo, and C. L. Chiu, Phys. Rev. B **62**, 14268 (2000).
[35] W. C. Lin, C. C. Kuo, C. L. Chiu, and M. T. Lin, Surf. Sci. **478**, 9 (2001).
[36] See Supplemental Material at http://link.aps.org/supplemental/10.1103/PhysRevB.94.064402 for information of the crystalline structure of Ni, Mn, and Co films and the procedure of obtaining the magnetic domain images with photoemission electron microscopy.
[37] M. Zheng, J. Shen, P. Ohresser, Ch. V. Mohan, M. Klaua, J. Barthel, and J. Kirschner, J. Appl. Phys. **85**, 5060 (1999).
[38] W. Platow, U. Bovensiepen, P. Poulopoulos, M. Farle, K. Baberschke, L. Hammer, S. Walter, S. Müller, and K. Heinz, Phys. Rev. B **59**, 12641 (1999).
[39] J. Hafner and D. Spišák, Phys. Rev. B **72**, 144420 (2005).
[40] J. Stöhr, Y. Wu, B. D. Hermsmeier, M. G. Samant, G. R. Harp, S. Koranda, D. Dunham, and B. P. Tonner, Science **259**, 658 (1993).
[41] C. M. Schneider and G. Schönhense, Rep. Prog. Phys. **65**, R1785 (2002).
[42] D.-H. Wei, Y.-L. Chan, and Y.-J. Hsu, J. Electron Spectrosc. Relat. Phenom. **185**, 429 (2012).
[43] J. Stöhr and H. C. Siegmann, *Magnetism: From Fundamentals to Nanoscale Dynamics*, illustrated ed. (Springer, New York, 2006).
[44] B. Y. Wang, C. H. Chuang, S. S. Wong, J. J. Chiou, W. C. Lin, Y. L. Chan, D. H. Wei, and M. T. Lin, Phys. Rev. B. **85**, 094412 (2012).
[45] B. Schulz and K. Baberschke, Phys. Rev. B **50**, 13467 (1994).
[46] J. Hong, R. Q. Wu, J. Lindner, E. Kosubek, and K. Baberschke, Phys. Rev. Lett. **92**, 147202 (2004).
[47] T. Burkert, O. Eriksson, P. James, S. I. Simak, B. Johansson, and L. Nordström, Phys. Rev. B **69**, 104426 (2004).
[48] J. Nogués and I. K. Schuller, J. Magn. Magn. Mater. **192**, 203 (1999).
[49] S. Roy, M. R. Fitzsimmons, S. Park, M. Dorn, O. Petracic, I. V. Roshchin, Z. P. Li, X. Batlle, R. Morales, A. Misra, X. Zhang, K. Chesnel, J. B. Kortright, S. K. Sinha, and I. K. Schuller, Phys. Rev. Lett. **95**, 047201 (2005).
[50] H. Ohldag, H. Shi, E. Arenholz, J. Stöhr, and D. Lederman, Phys. Rev. Lett. **96**, 027203 (2006).
[51] J. S. Park, J. Wu, E. Arenholz, M. Liberati, A. Scholl, Y. Meng, C. Hwang, and Z. Q. Qiu, Appl. Phys. Lett. **97**, 042505 (2010).
[52] Y. Meng, J. Li, A. Tan, E. Jin, J. Son, J. S. Park, A. Doran, A. T. Young, A. Scholl, E. Arenholz, J. Wu, C. Hwang, H. W. Zhao, and Z. Q. Qiu, Appl. Phys. Lett. **98**, 212508 (2011).
[53] Y. Meng, J. Li, A. Tan, J. Park, E. Jin, H. Son, A. Doran, A. Scholl, E. Arenholz, H. W. Zhao, C. Hwang, and Z. Q. Qiu, Phys. Rev. B **84**, 064416 (2011).
[54] P. J. van der Zaag, Y. Ijiri, J. A. Borchers, L. F. Feiner, R. M. Wolf, J. M. Gaines, R. W. Erwin, and M. A. Verheijen, Phys. Rev. Lett. **84**, 6102 (2000).
[55] J. van Lierop, K. W. Lin, J. Y. Guo, H. Ouyang, and B. W. Southern, Phys. Rev. B **75**, 134409 (2007).
[56] K. Lenz, S. Zander, and W. Kuch, Phys. Rev. Lett. **98**, 237201 (2007).
[57] T. Hagelschuer, Y. A. Shokr, and W. Kuch, Phys. Rev. B **93**, 054428 (2016).
[58] W. Kuch, F. Offi, L. I. Chelaru, M. Kotsugi, K. Fukumoto, and J. Kirschner, Phys. Rev. B **65**, 140408(R) (2002).
[59] T. Ambrose and C. L. Chien, Phys. Rev. Lett. **76**, 1743 (1996).